Electronic Supplementary Material (ESI) for Physical Chemistry Chemical Physics.
This journal is © the Owner Societies 2014

Supporting Information for:

Predictions of Voltage Dependence of Interfacial Electrochemical Processes at Lithium-Intercalated Graphite Edge Planes: Supporting Information

Kevin Leung

Sandia National Laboratories, MS 1415, Albuquerque, NM 87185

Contents

S1. Monte Carlo Details and Contact Ion Pairs

To generate a starting configuration for each AIMD trajectory, Monte Carlo (MC) simulations are conducted using the Towhee code[1] and simple, rigid classical force fields for LiC_6 edge plane atoms, EC, FEC^-, and/or PF_6^-. Each set of pre-equilibration simulation consists 'of three segments of 10^5 (MC) passes, conducted at successive temperatures of T=1050, 750, and 450 K. Molecular and electrode geometries in these MC simulations are taken from DFT optimization calculations. EC and Li^+ force field parameters are described in Refs. 2 and 3. Relevant partial charges and 12/6 Lennard-Jones parameters are listed in Table S1.

The main text states that "anode potential" ($\mathcal{V}(\sigma, n_{\rm Li})$, referenced to experimental Li^+/Li(s) value) validation calculations rely on FEC^- being well-separated from Li^+. The reason is as follows. We have found that Li^+/FEC^- contact ion pairs (CIPs) tend to dissociate in picosecond timescales during our T=450 K AIMD trajectories. The reduction potential (Φ) of isolated FEC^- and FEC^-:Li^+ CIPs are quite different; as soon as a CIP dissociates, FEC^-, which has been stable before, gives up its excess e^-. In reality, the separated ions may recombine to form CIPs at later times, and Li^+/FEC^- CIPs may exist with a statistically significant probability, especially at 1.0 M Li^+ concentration. However, AIMD trajectories are too short to sufficiently sample ion diffusion-related properties.

As a result, we only consider FEC^- not coordinated to Li^+. This allows us to compare our interfacial simulations in the main text with calculations of the reduction potential of FEC not coordinated to Li^+ (Sec. S3 below). While Φ for FEC reduction is lower than measured values, our focus is self-consistency in this work.

In Monte Carlo simulations that involve mobile Li^+ and FEC^-, even when the starting MC configurations do not contain contact ion pairs, CIPs are formed at the end of the trajectories. To prevent this, the centers-of-mass of FEC^- and mobile Li^+ are frozen in MC simulations. These constraints are removed during an additional, final MC run of 5000 passes at T=450 K, after which it is found that CIPs have not reformed. Note that simulations depicted in Fig. 1 of the main text do not involve anions, and CIP is not an issue there.

S2. Edge Plane Work Functions and Potential Estimate if Solvent is Omitted

In Ref. 3, the anode potentials of the C=O and C-OH edge plane terminated LiC_6 strips were determined using a solid state physics approach. Charge-neutral Li *atoms* were added to a charge-neutral LiC_6 edge plane until the last one was associated with a binding energy similar to Li metal cohesive energy. This approximates the condition of 0.0 V vs. Li^+/Li(s). The procedure seems reasonable for bulk electrode systems without surfaces, although interfacial contributions are missing and the predictions do not truly represent "open circuit potentials." But the method neglects the liquid electrolyte, making its use at electrode/electrolyte interfaces potentially unreliable.

molecule	FEC^-								PF_6^-		C=O	
atom	C_C	C_1	C_2	O_C	O_1	O_2	H	F	P	F	C	O
q	0.15	0.72	-.12	-.76	-.58	-0.27	-.39	0.08	1.61	-.44	var	-.66
ϵ	0.42	0.42	0.42	0.85	0.69	0.69	0.42	0.12	2.05	0.32	0.42	0.85
σ	3.75	3.75	3.75	2.96	3.00	3.00	3.03	2.50	3.83	3.03	3.43	3.00

TABLE S1: Partial atomic charge (q in units of $|e|$) and Lennard-Jones parameters (ϵ in kJ/mol and σ in Å) for FEC^-, PF_6^-, and edge plane C=O atoms. C_1 and O_1 are the ethylene carbon and oxygen atoms on the fluorine side while C_2 and O_2 are on the other side. The average q are listed for the 3 H atoms on FEC. Only the outermost carbon and oxygen edge atoms, and the Li^+ bound to them, are explicitly included in MC simulations. They are frozen in DFT-optimized geometry. Each edge carbon atom is assigned the same compensating q_C, which depends on n_{Li}, to make the simulation cell charge neutral. The interior of the electrode should be charge-neutral, as befits a metallic system.

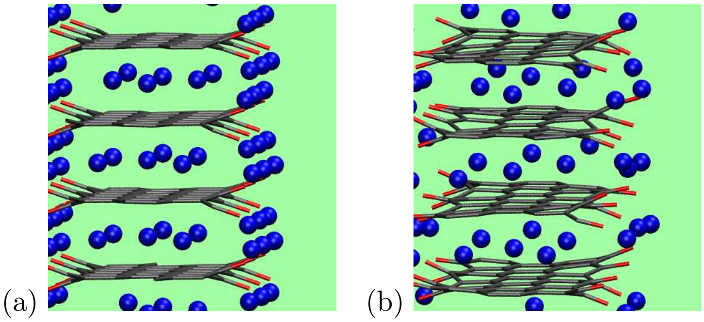

FIG. S1: DFT-optimized geometries of model LiC_6 anode with edge planes terminated in C=O groups. (a) n_{Li}=1.0; (b) n_{Li}=0.5. C, O, and Li atoms are depicted as grey, red, and blue spheres, respectively.

Using this surface science approach, $n_{Li} = 1$ and σ=0 with C=O edge terminations were assigned to ~0.0 V vs. Li^+/Li(s) in Ref. 3. In contrast, extrapolating to $n_{Li} = 1$ in Fig. 1a of the main text yields a much lower potential — more negative than Li^+/Li(s). Since Fig. 1 of the main text explicitly accounts for the liquid solvent, it should be more reliable. Therefore the solid state method used in Ref. 3 appears to severely underestimate the anode potential.

Next, we explore an alternate surface science method of estimating "potentials-of-zero-charge." We stress that it is only possible to calculate the potential in the absence of liquid electrolytes at zero surface charge. $\sigma \neq 0$ would have needed charge compensation in the liquid region — either using explicit salt models or via Poisson-Boltzmann and related approximations. When σ=0, the free energy of Li^+ transfer from the electrode to the bulk electrolyte ($\Delta G_t'$) is here estimated by assuming that interfacial effects were absent. The remaining contributions to $\Delta G_t'$ are listed in Table S2: (1) remove an Li atom from bulk LiC_6 to vacuum (i.e., Li atom vacancy energy); (2) $Li(g) \rightarrow Li^+(g) + e^-$ (Li gas phase ionization

n_{Li}	0.417	0.500	0.583	0.667	0.750	0.833	0.917	1.000
$\mathcal{W}$	3.720	3.180	2.770	2.520	2.351	2.140	1.810	1.468
$\Delta G_t'$	-2.36	-1.82	-1.41	-1.16	-0.99	-0.78	-0.45	-0.11
$\mathcal{V}'$	2.46	1.92	1.51	1.26	1.09	0.68	0.55	0.21

TABLE S2: Work functions ($\mathcal{W}$), and estimated voltage ($\mathcal{V}'(\sigma = 0, n_{\mathrm{Li}})$) if liquid-solid interfacial effects were absent, as functions of n_{Li}. Other contributions to $\mathcal{V}$ are Li vacancy in bulk $\mathrm{LiC_6}$ (1.65 eV), gas phase Li ionization potential (5.30 eV), $\mathrm{Li^+}$ solvation free energy (-5.20 eV)[3], and a -0.39 eV entropy correction for 1.0 M $\mathrm{Li^+}$ concentration and Li vibration in $\mathrm{LiC_6}$, all computed using DFT/PBE. $\mathcal{W}$ and $\Delta G_t'$ are in eV while $\mathcal{V}'$ are in units of volt.

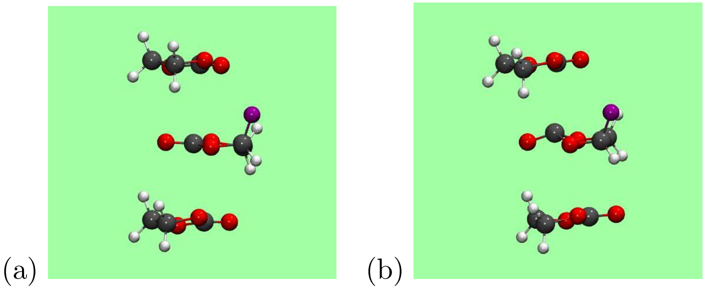
(a) (b)

FIG. S2: FEC geometries optimized using the PBE functional and a dielectric continuum approximation. (a) $\mathrm{(EC)_2FEC}$; (b) $\mathrm{(EC)_2FEC^-}$. Grey, red, white, and purple spheres depict C, O, H, and F atoms, respectively.

potential); (3) put the ionized e^- back into $\mathrm{LiC_6}$ (reverse of the work function $\mathcal{W}$); (4) $\mathrm{Li^+(g)} \rightarrow \mathrm{Li^+(EC)}$ ($\mathrm{Li^+}$ solvation free energy in bulk electrolyte). Using the PBE functional, the 0.39 eV entropic correction of the main text, and the solvation free energy computed in Ref. 4, steps 1,2, and 4 plus a 0.1 V conversion to the $\mathrm{Li^+/Li(s)}$ reference yield a combined 1.26 eV. This value is reasonably close to the widely quoted 1.37 eV reference used to shift the energy of an e^- in vacuum to the $\mathrm{Li^+/Li(s)}$ voltage.[5] The discrepancy is probably due to the use of the PBE functional.

Combining the 1.46 eV correction with $\mathcal{W}$ yields the potentials $\mathcal{V}'$ at at various n_{Li} (Table S2). Just like in the original surface science method described above,[3] $\mathcal{V}'(\sigma = 0, n_{\mathrm{Li}} = 1)$ is close to 0 V vs. $\mathrm{Li^+/Li(s)}$ (0.21 V). Compared with the extrapolation in Fig. 1a in the main text, $\mathcal{V}'(\sigma = 0, n_{\mathrm{Li}})$ is shifted to more positive voltages than $\mathcal{V}(\sigma = 0, n_{\mathrm{Li}})$. At n_{Li}=0.5, the shift is about 0.9 V. $d\mathcal{V}'(\sigma = 0, n_{\mathrm{Li}})/dn_{\mathrm{Li}}$ is also large than $d\mathcal{V}(\sigma = 0, n_{\mathrm{Li}})/dn_{\mathrm{Li}}$ by $\sim$ 25% in the range $0.42 < n_{\mathrm{Li}} < 0.58$.

This demonstrates the importances of accounting for electrolyte molecules at the interface even in the absence of ions. At water-metal interfaces, significant solvent-induced work function shifts have also been reported.[6,7]

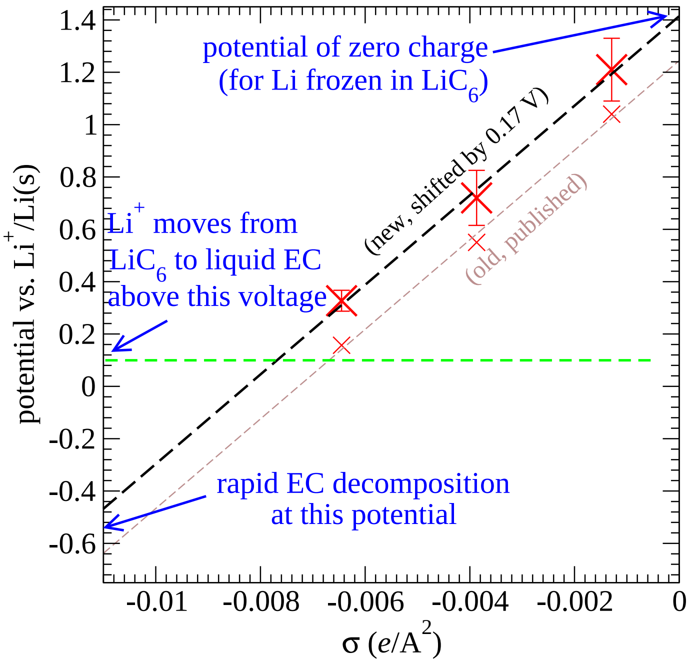

FIG. S3: “Anode voltage” on LiC_6 basal planes, referenced to Li^+/Li(s), as a function of surface charge σ. This figure is adapted from Ref. 4, but shifted to more positive voltages by 0.17 V (see the main text).

S3. FEC reduction potential

The FEC reduction potential (Φ) is needed to corroborate our anode potential calibration calculations. The model systems used are $(EC)_2FEC^{n-}$ clusters with n=0 and 1 (Fig. S2). As discussed in Sec. S1, no Li^+ is coordinated to FEC. We apply the PBE functional to be consistent with the AIMD/PBE simulations reported in main text, the gaussian code version g09,[8] a `6-31+G(d,p)` basis for optimization and thermal correction calculations, and a `6-311++G(3df,2pd)` basis for final single point enegy evaluation. The electrolyte surrounding the EC/FEC cluster is approximated using a dielectric continuum treatment[9] with ϵ=40 assumed.[5] Φ=0.58 V is predicted for the $(EC)_2$FEC cluster, as quoted in the main text. If the EC spectator molecules are omitted, and only a single FEC “solvated” by the dielectric continuum is used in calculations, Φ is predicted to be 0.51 V. The small discrepancy between the two cluster sizes derives almost entirely from thermal corrections, not from enthalpy changes.

When FEC is coordinated to Li^+ in a $Li^+FEC^{n-}(EC)_2$ cluster, Φ is predicted to be 0.77 V. This value is larger than the cluster model without Li^+ but still lower than the measured 0.95 V.[10] The discrepancy with measurements is likely due to errors associated with DFT/PBE. We stress that Fig. 2 of the main text is more concerned with obtaining

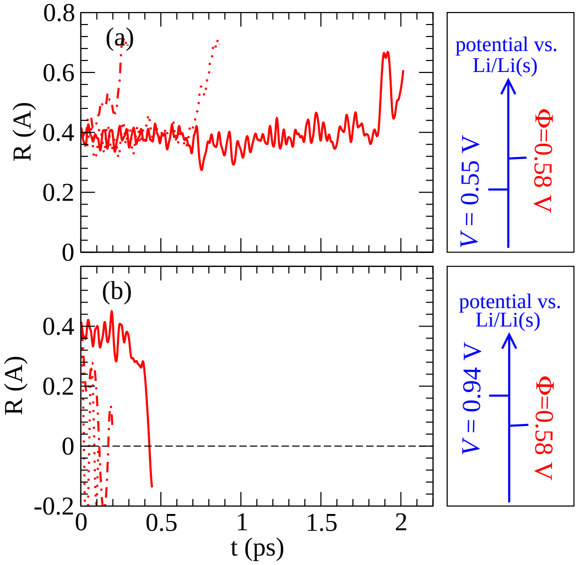

FIG. S4: (a)&(b) FEC carbonyl carbon (C_C) out-of-plane coordinate R (defined in the main text) as a function of time when the anode potential V is lower or higher than the bulk FEC reduction potential Φ, respectively. The different line shapes indicate 3 trajectories with different initial configurations.

internal consistency of the potential calibration scheme than with accuracy compared with measurements. Agreement with experimental values can be improved by post-processing single point corrections of DFT/PBE predictions using more sophisticated DFT functionals or quantum chemistry methods.

S4. Basal Plane Potential Validation

We have also carried out validation calculations of “anode potentials” previously predicted for LiC_6 basal planes. In Fig. S3, $\mathcal{V}(\sigma)$ values are adapted from Ref. 4, but are shifted to more positive potentials by 0.17 V to reflect our modified entropy estimates (see the main text). Note that there are no surface pockets to retain Li^+ on basal planes, and the potential is a function of the surface electronic charge density only. Using Fig. S3 to calibrate the anode potential, we examine the stability of FEC^- near LiC_6 basal planes, analogous to the calculations depicted in Fig. 2 of the main text for edge planes. Fig. S4 shows that, when this basal plane $\mathcal{V}(\sigma)$ is more negative than the FEC reduction potential Φ, FEC^- retains its excess e^-. When $\mathcal{V}(\sigma)>\Phi$, FEC^- loses its excess e^-. We have conducted three simulations under each voltage condition with different starting configurations generated by MC pre-equilibration, and the qualitative outcomes are reproduced each time. This demonstrates the reliability of our potential calibration scheme at basal plane interfaces.

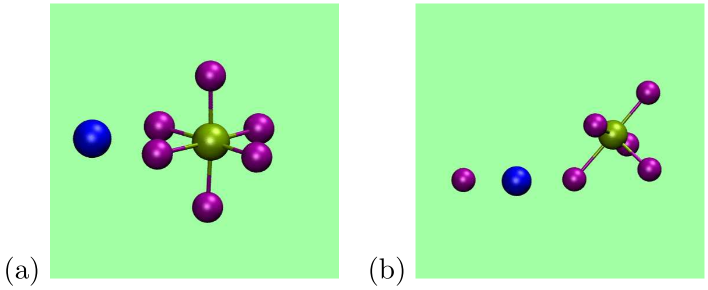

FIG. S5: DFT-optimized geometries of (a) Li^+/PF_6^- pair; (b) Li^+/PF_5^-+F^-. P, F, and Li atoms are depicted as lime-green, purple, and blue spheres, respectively.

S5. Reductive Decomposition of Li^+/PF_6^- Cluster

Fig. S5a depicts the geometries of an intact Li^+/PF_6^- contact ion pair, optimized using DFT/PBE with a `6-31+G(d,p)` basis in a SMD dielectric continuum with ϵ=40. Fig. S5b depicts an electrochemically reduced Li^+/PF_5^- pair with one F^- detached from the P-atom; the P atom now contains an unpaired e^-. The free energy change of the reaction, including thermal corrections, is -2.83 eV.[11] After adding the standard 1.37 eV which is the cost of an e^- when using the Li^+/Li(s) reference, an apparent reduction potential of 1.46 V is obtained. Adding explicit solvent molecules may improve the accuracy but is not expected to qualitatively alter these predicted values.

However, adding an e^- to the ion pair of Fig. S5a does not spontaneously trigger decomposition in the geometry optimization calculations. To arrive at panel (b), one of the P-F bonds has to be manually and significantly elongated in the starting configuration. Partially cleaving the P-F bond thus appears a prerequisite for e^- injection. This suggests that a significant kinetic barrier may exist, which may translate into an overpotential required for electrochemical reduction. Indeed, to our knowledge, no cyclic voltametry measurement has reported a ∼1.5 V peak associated with electrochemical reduction of PF_6^--based electrolyte. It is more likely that, if PF_6^- reacts electrochemically occur at all, an excess e^- first finds its way into solvent molecules like EC and then attacks PF_6^-, in solvent-assisted pathways reminiscent of oxidative decomposition of electrolytes.[12]

In conclusion, inside bulk liquid-electrolytes, reductive decomposition of Li^+/PF_6^- is thermodynamically favorable but does not proceed spontaneously. Solvent-assisted routes are currently being investigated. This provides the background and context for predicting PF_6^- decomposition free energies right at LiC_6 edge planes, discussed in the main text and the next section of this S.I.

	n_{Li}	B	R_o	T	decomp
K	0.583	0.0	0.0	9.6	no
L	0.583	0.1	1.0	12.0	no
M	0.583	0.4	2.5	12.4	no
N	0.583	0.7	2.5	12.1	no
O	0.750	0.0	0.0	9.4	no
P	0.750	0.1	1.0	6.2	EC
Q	0.750	0.4	2.5	1.2	PF_6^-

TABLE S3: Details of AIMD trajectories used in potential-of-mean-force ($\Delta W(R)$) calculations (Fig. 4a of the main text). Two PF_6^- reside on the edge planes, charge-compensated with mobile Li^+ ions. B and R_o are in units of eV and Å respectively. The reaction coordinate R' (which roughly tracks R_o in the constraining potetial) should be at least 1 Å when the designated P-F bond is broken.

S6. PF_6^-: AIMD potential-of-mean-force details

AIMD-based potential-of-mean-force (PMF) simulations of PF_6^- decomposition are initiated using MC simulations with one PF_6^- at each edge plane of the LiC_6 slab, with two mobile Li^+ compensating their charges. MC pre-equilibration is performed as described in Sec. S1, except that centers-of-mass of the two PF_6^- are frozen during the T=1050 K MC run but are allowed to move during T=750 K and T=450 K MC simulations. The anions remain close to the electrode surface during these lower temperature trajectories. The P atom and a F atom on one of the PF_6^-, and the Li at the electrode edge to which the selected F is coordinated, are used henceforth in the definition of reaction coordinate R':

$$R' = |\mathbf{R}_{\mathrm{P}} - \mathbf{R}_{\mathrm{F}}| - |\mathbf{R}_{\mathrm{Li}} - \mathbf{R}_{\mathrm{F}}|.$$

Seven trajectories are conducted while imposing constraining umbrella sampling potentials of the form $U(R') = B(R' - R_o)^2$. See Table S3 for details. Trajectories P and Q, estimated to occur at -0.21 V vs. $Li^+/Li(s)$, have to be truncated because irreversible EC and PF_6^- decompositions have occurred, respectively. Due to its short duration, Q is not used in Fig. 4 of the main text at all.

---

[1] Martin, M.G.; Thompson, A.P. Industrial Property Prediction using Towhee and LAMMPS. *Fluid Phase Equil.* **2004**, *217*, 105-110.

[2] Li, T.; Balbuena, P.B. Theoretical Studies of Lithium Perchlorate in Ethylene Carbonate, Propylene Carbonate, and their Mixtures. J. Electrochem. Soc. **146**, 3613 (1999); Marquez, A.; Balbuena, P.B. Molecular Dynamics Study of Graphite/Electrolyte Interfaces. J. Electrochem. Soc. **148**, A624 (2001).

[3] Leung, K.; Budzien, J.L. *Ab initio* Molecular Dynamics Simulations of the Initial Stages of Solid-Electrolyte Interphase Formation on Lithium Ion Battery Graphitic Anodes. *Phys. Chem. Chem. Phys.* **2010**, *12*, 6583-6586.

[4] Leung, K.; Tenney, C.M. Towards First Principles Prediction of Voltage Dependences of Electrode/Electrolyte Interfacial Processes in Lithium Ion Batteries. *J. Phys. Chem. C* **2013**, *117*, 24224-24235.

[5] Leung, K. Two-electron Reduction of Ethylene Carbonate: a Quantum Chemistry Reexamination of Mechanisms. *Chem. Phys. Lett.* **2013**, *568-569,* 1-8.

[6] Schnur, S.; Gross, A. Properties of Metal-Water Interfaces Studied from First Principles. *New J. Phys.* **2009**, *11*, 125003.

[7] Cheng, J.; Sprik, M. Alignment of Electronic Energy Levels at Electrochemical Interfaces. *Phys. Chem. Chem. Phys.* **2012**, *14*, 11245-11267.

[8] Gaussian 09, Revision A.1, M.J. Fritsch *et al.*, Gaussian, Inc., Wallingford CT, 2009.

[9] Marenich, A.V.; Cramer, C.J.; Truhlar, D.G. *J. Phys. Chem. B* **2009**, *113*, 6378.

[10] Wang, Z.; Xu, J.; Yao, W.-H.; Yao, Y.-W.; Yang, Y. Fluoroethylene Carbonate as an Electrolyte Additive for Improving the Performance of Mesocarbon Microbead Electrode. *ECS Trans.* **2012**, *41*, 29.

[11] If the B3LYP functional is used, the value is -2.89 eV, similar to the DFT/PBE prediction of -2.83 eV.

[12] Xing, L.; Borodin, O.; Smith, G.; Li, W. Density Functional Theory Study of the Role of Anions on the Oxidative Decomposition Reaction of Propylene Carbonate. *J. Phys. Chem.* **2011**, *115*, 13896-13905.